IOVS Papers in Press. Published on August 12, 2014 as Manuscript iovs.14-14421

# Loss of outer retinal neurons and circuitry alterations in the DBA/2J mouse

Laura Fernández-Sánchez[1], Luis Pérez de Sevilla Mueller[2], Nicholas C. Brecha[2-6] and Nicolás Cuenca[1]

[1]Department of Physiology, Genetics and Microbiology, University of Alicante, San Vicente del Raspeig, Spain;

[2] Department of Neurobiology, [3] Department of Medicine, [4] Jules Stein Eye Institute, [5] CURE Digestive Diseases Research Center, David Geffen School of Medicine at Los Angeles, University of California at Los Angeles, Los Angeles, California 90095-1763, USA. [6] Veterans Administration Greater Los Angeles Health System, Los Angeles, California 90073, USA

**Running title:** DBA/2J outer retina degeneration

**Key words:** photoreceptor, horizontal cell, bipolar cell, synaptic triad, retinal degeneration, glaucoma.

**Associate Editor: Elke Luetjen-Drecoll**

**Corresponding author**:

Dr. Nicolás Cuenca
Department of Physiology, Genetics and Microbiology
University of Alicante
San Vicente del Raspeig E-03690, Spain.
Phone: +34965903856
Fax: +34965903943
E-mail: cuenca@ua.es

**Precis: This study using specific synaptic and cellular markers shows an impairment of the outer retina in the DBA/2J mouse retina starting at 3 months of age.**

**Pages: 27**

**Word count: 4442**

**Figures:8**

**Support or grant information**

This research was supported by grants from the Spanish Ministry of Economy and Competitivity- FEDER (BFU2012-36845), Instituto de Salud Carlos III (RETICS

RD12/0034/0010), National Organization of Spanish blind (ONCE) (ONCE1-13I), FUNDALUCE, NIH EY04067 (NCB), NIDDDK P30 DK41301 (UCLA Cure Center Core) and a VA Merit Review (NCB). NCB is a VA Career Research Scientist.

**Abstract (250 words)**

**Purpose:** The DBA/2J mouse line develops essential iris atrophy, pigment dispersion, and glaucomatous age-related changes, including an increase of intraocular pressure, optic nerve atrophy and retinal ganglion cell death. The aim of this study was to evaluate possible morphological changes in the outer retina of the DBA/2J mouse concomitant with disease progression and aging, based on the reduction of both the a- and b-waves and photopic flicker ERGs in this mouse line.

**Methods:** Vertically sectioned DBA/2J mice retinas were evaluated at 3, 8 and 16 months of age using photoreceptor, horizontal and bipolar cell markers. Sixteen month old C57BL/6 mice retinas were used as controls.

**Results:** DBA/2J mice had outer retinal degeneration at all ages, with the most severe degeneration in the oldest retinas. At 3 months of age, the number of photoreceptor cells and the thickness of the OPL were reduced. In addition, there was a loss of horizontal and ON-bipolar cell processes. At 8 months of age, RGC degeneration occurred in patches, and in the outer retina overlying these patches, cone morphology was impaired with a reduction in size as well as loss of outer segments and growth of horizontal and bipolar cell processes into the outer nuclear layer. At 16 months of age, connectivity between photoreceptors and horizontal and bipolar cell processes overlying these patches was lost.

**Conclusions:** DBA/2J retinal degeneration includes photoreceptor death, loss of bipolar and horizontal cell processes, and loss of synaptic contacts in an aging-dependent manner.

## Introduction

Glaucoma is a heterogeneous group of chronic ocular diseases in which retinal ganglion cells (RGC) die by apoptosis[1,2]. Glaucoma is the second most frequent cause of blindness in the worldwide representing 8% of all cases, according to the World Health Organization[3]. Angled-closure glaucoma usually develops an increase in intraocular pressure (IOP) leading to optic nerve damage, RGC death and a permanent loss of vision[2]. The DBA/2J mouse line[4,5,6] has been suggested as a secondary angle-closure glaucoma model because of its closely resemblance to this type of human glaucoma[7]. At 3 to 6 months of age, the DBA/2J mouse eye begins to develop essential iris atrophy, pigment dispersion, and glaucomatous age-related changes, including an increase of IOP, optic nerve atrophy and RGC death. The DBA/2J mouse line carries recessive mutations in genes encoding, glycosylated protein nmb (Gpnmb; NCBI GeneID 93695) and tyrosinase-related protein 1 (Tyrp1; NCBI GeneID 22178)[8,9]. Mice with these mutations spontaneously develop iris atrophy, pigment deposition in the anterior segment and eventually blockage of ocular drainage structures[8], elevated IOP, optic nerve atrophy and RGC degeneration, usually by apoptosis[8,9]. This ocular pathology may begin as early as three months of age[10]. Previous studies have evaluated and documented RGC degeneration and reduction of the inner retina concomitant with aging and disease progression in the DBA/2J mouse line[10–12].

Electroretinograms (ERGs) performed on young DBA/2J mice (2-3 months) showed that both, the oscillatory potentials and photopic flicker ERGs, are lower than those from age matched C57BL/6 mice[13], whereas scotopic ERG responses had similar amplitudes in their a- and b-waves[13,14]. However, older DBA/2J mice (195 to 305 days) have lower amplitudes in their a- and b-waves compared to C57BL/6 mice[13]. Furthermore, a significant reduction of the scotopic a- and b-wave amplitudes has also been reported for two-year-old DBA/2J mice[15], suggesting changes in the functional

integrity of the outer retina, since these waves are mainly generated by photoreceptor and ON bipolar cell responses[16,17]. Fuchs and cols [18] found a narrowing of the OPL that they attribute to structural synaptic ribbon impairment in the axon terminal of rod photoreceptors. However, there is poor information available regarding cellular or synaptic changes in the outer retina of the DBA/2J line with aging and disease progression that could account for these changes in the ERG. In this study, we have evaluated the cellular morphology of the outer nuclear layer (ONL) and the organization of the outer plexiform layer (OPL) of the DBA/2J mouse retina at different ages, before and after the onset of RGC degeneration.

## Materials and Methods

*Animals and tissue preparation*

DBA/2J (*Gpnmb*$^{R150X}$ and *Tyrp1*$^{isa}$) mice female at 3, 8 and 16 months old, with a total of 12 animals, were used in this study. C57BL/6 mice female at 16 months old were used as controls. Animals were obtained from the Jackson Laboratory (Bar Harbor, ME, USA) and they were maintained and bred in temperature and light controlled rooms with a 12 hours light/dark cycle and had food and water ad libitum at the David Geffen School of Medicine at the University of California, Los Angeles (UCLA). DBA/2J is a well-studied secondary angle-closure glaucoma model presenting IOP increase. The IOP measurements reported by others and us showed increased IOP in this model starting around 6 months-old and is maintained with aging[4,12]. All experiments were performed in accordance with the guidelines and policies for the welfare of experimental animals established by the U.S. Public Health Service Policy on Human Care and Use of Laboratory Animals (2002), the UCLA Animal Research Committee, and the ARVO Statement for the Use of Animals in Ophthalmic and Vision Research. The mice were deeply anesthetized with 1-3% isofluorane (Novaplus, Lake Forest, IL). The eyes were enucleated and fixed in cold 4% paraformaldehyde in 0.1 M phosphate saline buffer (PBS), pH 7.4, for 60 minutes at room temperature (RT). Eyes were immersed in 15 and then 20% sucrose in PBS for one hour each, and left in 30% sucrose in PBS overnight at 4°C. The following day, the cornea, lens and vitreous body were removed and embedded in Tissue-Tek OCT (Sakura Finetek, Zoeterwouden, Netherlands) and frozen in liquid $N_2$. Vertical sections of the retina were cut at 16 µm thickness on a cryostat (Leica CM 1900, Leica Microsystems) in a horizontal plane, and mounted on Superfrost Plus slides (Menzel GmbH & Co KG, Braunschweig, Germany), and air-dried.

*Immunohistochemistry*

For immunohistochemistry, at least three animals were studied at each time point. Retinas from C57BL/6 and DBA/2J mice were processed in parallel, and retinal sections were treated as in previous studies[19–22]. Briefly, the sections were thawed and washed 3x10 minutes in 0.1 M PB, pH 7.4, and then incubated in blocking solution (10% normal donkey serum in 0.1 M PB containing 0.5% Triton X-100) for 1 hour at RT in the dark. The sections were then incubated in the primary antibodies diluted in PB containing 0.5% Triton X-100 overnight at RT. All primary antibodies used in this work (summarized in Table 1) had been utilized in several previous studies and are well characterized by others and us regarding cell type specificity. The sections were subsequently washed in PB and incubated in the corresponding secondary antibodies at a 1:100 dilution for 1 hour at RT. Secondary antibodies used in this work were Alexa Fluor 488–anti-rabbit IgG, Alexa Fluor 555–anti-mouse IgG donkey and Alexa Fluor 633–anti-guinea pig IgG donkey (Invitrogen, Carlsbad, CA). The nuclear marker, TO-PRO-3 iodide (Invitrogen) was added at 1 $\mu$M with the secondary antibodies. The sections were finally washed 3x10 minutes in PB, mounted in Citifluor (Citifluor Ltd; London, UK) and cover slipped for viewing with a Leica TCS SP2 laser-scanning confocal microscope. To control for non-specific staining, some sections were processed without the primary antibody. Final images from C57BL/6 and DBA/2J retinas were processed in parallel using the Adobe Photoshop 10 software (PhotoShop 10; Adobe, San Jose, CA).

*Morphometric analysis.*

ONL measurements were performed on retinal sections stained with TO-PRO 3-iodide. Sections stained with antibodies against calbindin at different ages were used to quantify the invaginated terminal tips of horizontal cell into the photoreceptor axon terminals. All measurements were taken in the central area, near the optic nerve head, of at least 3 animals in 8 single scanned pictures at each eye and age-point. At 8 and

16 months, digital images were taken inside and outside the patches. The patches in retinal sections were defined as areas with greater loss of photoreceptor cells, decreased synaptic connectivity in the OPL with high diminution in the horizontal cell plexus. In addition, it was possible to find inside these areas vascular alterations in the superficial plexus together with retinal remodelation (Figure 4 and supplementary material S1). ImageJ software (National Institutes of Health, Bethesda, MD, USA) was used for the morphometric analysis of the confocal images; the quantification of horizontal cell tips was done manually using the cell counter plugin.

*Statistical analyses*

Results were analyzed by Graphpad Prism (GraphPad Software, Inc. La Jolla, CA 92037 USA). For statistical analysis two-tailed Student's t-test was performed to compare the ONL thickness and the number of horizontal cell tips found at each age-point compared with control retina. P values of less than 0.05 were considered to be statistically significant.

## RESULTS

### Retinal thickness in the DBA/2J mice

The thickness of the outer and inner nuclear layers was evaluated using a nuclear stain, TO-PRO 3-iodide. Measurements were made on vertical sections central retina, 100 microns from the optic nerve head. In vertical sections of 16 month old C57BL/6 retinas, the ONL consisted of 12-14 rows of photoreceptor cell bodies, the inner nuclear layer (INL) consisted of 5 rows of cell bodies and there was a regular distribution of cells including RGCs in the ganglion cell layer (GCL) (Fig. 1A). In 3 month old DBA/2J retinas, the thickness of both nuclear layers appeared normal compared with C57BL/6 retinas, although there were some subtle alterations in the OPL, including misplaced nuclei resulting in discontinuities in the thickness of the OPL (Fig. 1B). These observations in the OPL at 3 months are consistent with findings from a previous report[18]. At 8 months old, the ONL was reduced to 9-11 rows of photoreceptor cell bodies and the INL was about 4 cellular rows (Fig. 1C). Quantification of ONL thickness showed a statistically significant reduction of about 20 microns in DBA/2J mice compared to C57BL/6, which can be converted in the loss of about 3-4 photoreceptor rows (Fig. 1E). The width of the OPL and IPL, at this age, was noticeably thinner than the OPL and IPL in the control retinas, and there was a marked reduction in cell number in the GCL (Fig. 1C). At 16 months of age, DBA/2J mice displayed a high variability between different animals in the ONL thickness. We found a reduction of 6 to 7 rows of photoreceptor cell bodies, the quantification showed a statistically significant reduction compared with C57BL/6 retinas (Fig. 1E). Furthermore, the reduction in the OPL and IPL thickness was evident, and in some areas, the OPL was difficult to identify (Fig. 1D, arrows).

**Alterations in the connectivity at the OPL level**

The photoreceptor synaptic triad[23–25] consists of a rod or cone axon terminal characterized by a synaptic ribbon, and two horizontal processes and a bipolar dendrite that invaginate the axonal terminal.

*Connectivity between photoreceptor and rod bipolar cells*

To evaluate the distribution of rod bipolar cell dendrites in rod synaptic triads, we performed double label immunostaining using antibodies against PKC-α, for rod bipolar cells, and Bassoon, a marker of the arciform density underlying the synaptic ribbon[26] (Fig. 2). In C57BL/6 retinas at 16 month old (Fig. 2A-C), the outer retina appeared to have a normal morphology, with bipolar cell dendrites terminating near Bassoon immunoreactive puncta, which demark the photoreceptor synaptic ribbon (Fig. 2A-C). In 3 month old DBA/2J retinas (Fig. 2D-F), the rod bipolar cell dendrites (green, Fig. 2D) were retracted with shorter tips compared to bipolar cells in C57/Bl retinas, and there was a significant decrease of Bassoon immunoreactive puncta (red, Fig. 2E). These anatomical changes are more apparent at older ages. In 8 month old DBA/2J retinas (Fig. 3G-I), most rod bipolar cells lacked dendrites, although there were a few dendrites that extended into the ONL (Fig. 2G). In addition, there were few Bassoon immunostained puncta (Fig. 2H) compared to earlier ages, and some of these puncta were not associated with bipolar dendrites (Fig. 2I, arrowhead), whereas other Bassoon immunoreactive puncta were localized at the end of dendrites in the ONL (Fig. 2I, arrow), indicative of a retraction of the rod spherules. In 16 month old DBA/2J retinas, only a few bipolar cell dendrites remained (Fig. 2J) and there was an overall reduction of Bassoon immunoreactive puncta (Fig. 2K-L).

*Connectivity between photoreceptors and horizontal cells*

To identify horizontal cell axons and dendrites we used an antibody to calbindin[27] (Fig. 3A,C). Photoreceptor axonal terminals were identified using an antibody to synaptophysin, a protein associated with synaptic vesicles[28] (Fig. 3B,C).

C57BL/6 retinas at 16 months old showed a regular distribution of horizontal cell dendritic tips and synaptophysin staining in rod and cone photoreceptor axon terminals associated with horizontal cell endings (Fig. 3A-C). In 3 month old DBA/2J retinas (Fig. 3D-F), there was a shortening of horizontal cell processes and a clear reduction of horizontal cell endings (Fig. 3D, arrowheads) compared with C57BL/6 retinas (Fig. 3A, arrowheads); although, the expression of synaptophysin immunostaining in the photoreceptor axon terminals (Fig. 3E) appear to remain at the same level as control retinas (Fig. 3B). In 8 month old DBA/2J retinas (Fig. 3G-I), the loss of horizontal cell processes and tips were more apparent (Fig. 3G, I, arrowheads) compared to control retinas (Fig. 3A, arrowheads). The staining of photoreceptor axon terminals with synaptophysin showed only 1 to 2 rows at the OPL at this age (Fig. 3H-I). In 16 month old DBA/2J retinas (Fig. 3 J-L), there was a discontinuous plexus of horizontal cell processes in the OPL with few endings (Fig. 3J, L), as well as a reduction of the photoreceptor axon terminals (Fig. 3K, H).

**Degeneration in retinal "patches"**

At 6-8 months of age in the DBA/2J retina, degeneration and loss of cells in the GCL is apparent [4,10,11] and located in discontinuous retinal areas[29]. Over time, these areas of RGC loss expand to cover most of the retina (See supplementary materials S2).

In retinal sections, we identified areas with changes in the inner and outer retina, which were referred to as "patches" compared to other areas in the same retinal section (Fig. 4). These patches (Fig. 4C) are areas where photoreceptors are lost and the OPL and INL presents alterations with a substantial decrease in the horizontal cell plexus (See supplementary materials S1), increased retraction of photoreceptor cell axons

accompanied by sprouting of horizontal and bipolar cells (Fig. 4A, C; arrowheads). Inside these areas it is possible to find vascular alterations (Fig. 4A, C; arrows) compared to neighbor areas with normal appearance (Fig. 4B, D).

*Cone photoreceptors*

To evaluate cone photoreceptor morphology, retinal sections were immunostained with an antibody against γ-transducin, a specific marker for cone photoreceptors [30]. To avoid the differences in cone density in different areas of the retina, the photographs for cone morphology studies were taken in the temporal area near optic nerve and inside the patches in all animals. The morphology of cone photoreceptors was well preserved in the DBA/2J retina at 3 (Fig. 5B), 8 and 16 months of age outside of the patches (Fig. 5C, E). In C57BL/6 retina at 16 months of age, the nuclei of cone photoreceptor cells were located in the distal ONL (Fig. 5A). In the DBA/2J retina at 3 months of age, some cone nuclei were located in the middle of the ONL (Fig. 5B, arrows). At 8 months of age there were patches with a greater degeneration compared to other areas of the retina. There was a marked loss of rows of photoreceptor cell bodies in the ONL in these regions. Cone photoreceptor morphology was altered, with an overall reduction in length, shorter outer segments (OS) and swollen inner segments (IS) (Fig. 5D, arrowheads). At 16 months of age, cone morphology was markedly impaired (Fig. 5F) compared with outer retinal regions that overlay retinal regions with RGCs (Fig. 5E). At this age, most cone photoreceptor cells lacked an obvious axon terminal (Fig. 5F, double arrowhead) and only a few cone photoreceptor cells were observed having a short axonal terminal (Fig 5F, arrows). In addition, the cone IS were swollen (arrowheads) and the OS were quite small (Fig. 5F), compared with control retinas (Fig. 5E).

*Bipolar cells*

Guanine nucleotide-binding protein β3 (GNB3), an isoform of the β subunit of a G-protein commonly associated with transmembrane receptors, is expressed by cone photoreceptors, and ON cone and ON rod bipolar cells [31]. Therefore, we used an antibody against GNB3 to evaluate bipolar cell morphology in the C57BL/6 and DBA/2J retinas (Fig. 6). In 3 month old DBA/2J retinas, GNB3 immunostaining showed a slight reduction of the bipolar cell dendrites (Fig. 6B, arrowheads) and the bipolar axon terminals in the IPL appeared to be less frequent and swollen compared with bipolar cells in C57BL/6 (Fig. 6A). In 8 month old DBA/2J retinas, a few GNB3 immunostained bipolar cell dendrites were present in middle of the ONL (Fig. 6C, D; arrows). The IPL was thinner at this age, and there were fewer bipolar cell axon terminals that were smaller than the bipolar cell axonal terminals in the C57BL/6 retina. In 16 month old DBA/2J retinas, a greater number of bipolar cell dendrites showed growth into the ONL (Fig. 6E, arrows). In addition, at this age, bipolar cell bodies were disorganized in the INL, and there was a loss of axonal terminals and lateral varicosities in the IPL, especially over regions of RGC loss (Fig. 6F).

*Synaptic connectivity between photoreceptor and horizontal cells*

To evaluate alterations in the synaptic connectivity between photoreceptors and horizontal cells in the OPL, we performed triple immunostaining studies using markers for photoreceptor axonal terminals, the photoreceptor synaptic ribbon and horizontal cell processes. Antibodies against the vesicular glutamate transporter type 1 (VGLUT1), which transports glutamate into synaptic vesicles [32], was used to visualize cone and rod axon terminals. To identify the synaptic ribbon in the photoreceptor axon terminal, antibodies were used to detect the C-terminal binding protein 2 (CtBP2), which is domain B of RIBEYE, a structural protein of synaptic ribbons [33–35]. Antibodies to calbindin were used to visualize horizontal cell processes (Fig. 7). In the C57BL/6 retina (Fig. 7A), VGLUT1 immunostaining showed 3-4 rows of rod spherules in the OPL, and each rod spherule contained a synaptic ribbon, identified by CtBP2

314 immunoreactive puncta adjacent to the tip of the horizontal cell ending (Fig. 7A). In 3
315 month old DBA/2J retinas (Fig. 7B), there was a small reduction in the thickness of the
316 OPL compared to the C57BL/6 retinas (Fig. 7A). The quantification of the number of
317 horizontal cell showed a reduction of 10% compared to C57BL/6 retinas (Fig. 7G). In 8
318 and 16 month old DBA/2J retinas, the loss of connectivity between photoreceptors and
319 horizontal cells endings were evident (Fig. 7C, E). There was a loss of about 40% and
320 48% of the horizontal cell tips at 8 and 16 months, respectively over the retinal regions
321 with RGCs (Fig. 7G). In contrast, in outer retinal regions overlying regions of RGC loss
322 ("patches") at 16 months the decrease in the number of horizontal cell tips was about
323 80% (Fig. 7G), and only a very few horizontal cell tips, axonal terminals and
324 photoreceptor ribbons were identified (Fig. 7F). In addition at 8 and 16 months,
325 overlying regions where retinal ganglion cell remain, a few horizontal cell tips were
326 observed in the ONL indicating growth into the photoreceptor nuclear layer (Fig. 7C,
327 E). No VGLUT1 immunoreactivity was present in the axon terminals (Fig. 7C, E,
328 arrowheads), although the pairs between horizontal cell tips (calbindin, green) and
329 photoreceptor ribbons (CtBP2, red) were still present.
330
331 Similar findings were observed at 8 month inside the patches (Fig. 7D). At 16 months
332 of age, no horizontal cell bodies were found in regions above the "patches" and there
333 was a corresponding loss of the horizontal cell plexus in the OPL. In these regions, a
334 reduction of calbindin and CtBP2 immunoreactive puncta were evident (Fig. 7F,
335 arrows). In addition, CtBP2 and VGLUT1 immunoreactivity were found in the inner and
336 outer segments of the photoreceptors (Fig. 7F, arrowheads), instead of in the
337 photoreceptor axon terminal.
338 To determine if horizontal cell processes are in apposition to photoreceptor terminals
339 near the synaptic ribbon, and verify whether postsynaptic contacts with horizontal cells
340 were lost, we performed double label immunostaining with antibodies against CtBP2
341 (Fig. 8, red), and against syntaxin 4 (Fig. 8, green), a marker of horizontal cell tips [36].

342 The typical horseshoe morphology corresponding to photoreceptor ribbons in rod
343 spherules is associated with horizontal cell tips (Fig. 8A, arrowheads) and the disk-like
344 morphology corresponding to photoreceptor ribbons in cone pedicles are also
345 associated with horizontal cell dendrites (Fig. 8A, arrows).
346
347 In 3 month old DBA/2J retinas (Fig. 8B), there was a clear decrease of photoreceptor
348 ribbons together with a loss of their horseshoe morphology compared with C57BL/6
349 retinas (Fig. 8A). Some of the CtBP2 puncta observed were lacking their corresponding
350 syntaxin 4 immunoreactive spot (Figure 8B, arrowheads). In 8 month old DBA/2J
351 retinas, there was a reduction of the CtBP2 and syntaxin 4 pairs. In addition, the
352 horseshoe morphology of the ribbon changed to a small immunoreactive puncta and
353 pairs of CtBP2 and syntaxin 4 immunoreactive puncta were rare (Fig. 8C, arrowheads).
354 These changes were more evident in outer retinal regions above the patches of RGC
355 loss (Fig. 8D, arrowheads). The impairment of synaptic contacts was more evident at
356 16 months of age (Fig. 8E), where there were many examples of CtBP2
357 immunoreactive puncta without a corresponding syntaxin 4 immunoreactive puncta
358 (Fig. 8E, arrowheads). In outer retinal regions over the patches lacking RGCs at 16
359 months old, the pairs CtBP2 and syntaxin 4 in the OPL were infrequent. Only sporadic
360 pairs can be recognized (Fig. 8F, arrow). Some CtBP2 puncta were located in the
361 ONL and were not associated with syntaxin 4 immunoreactivity (Fig. 8F, arrowhead)
362
363 *Photoreceptor axon terminal morphology*
364 Neurotransmitter release requires ATP for synaptic vesicle release, which is generated
365 by large mitochondrion in the rod photoreceptor terminals [33,37–39]. To study the
366 energetic conditions of the photoreceptor axon terminals we used antibodies against
367 Cytochrome C (Cyt C) as a marker of mitochondrion. VGLUT1 and calbindin
368 antibodies were used to visualize rod spherules and cone pedicles, and horizontal cell
369 endings, respectively. In the C57BL/6J mouse retina at 16 months of age, rod

spherules express VGLUT1 immunoreactivity, and the horizontal endings in the synaptic triad can be easily recognized (Fig. 9A, inset, arrow). The giant mitochondrion expressing Cyt C immunoreactivity (Fig. 9, blue) was also visualized in the rod spherules [39]. In 3 month old DBA/2J retinas, VGLUT1 immunoreactivity was absent in some of the photoreceptor axon terminals, which were identified by the presence of punctae Cyt C immunostaining (Fig. 9B, arrows, inset, arrow). In 8 month old DBA/2J retinas, there was a widespread loss of VGLUT1 immunostaining in the photoreceptor axon terminals. Horizontal cell processes extended to the vicinity of the mitochondria in the ONL, and these regions of the photoreceptor lacked VGLUT1 immunoreactivity (Fig. 9C, arrows). Some horizontal cell endings ramified in the ONL and were isolated from photoreceptor axon terminals and mitochondria (Fig. 9C, arrowheads). Horizontal cell endings in the rod spherules were not present (Fig. 9C, inset) and the rod spherules containing VGLUT1 immunoreactivity were reduced in size. All of these morphological changes were more prominent in regions of the outer retina overlying patches of the inner retina lacking RGCs (Fig. 9D, inset).

In 16 month old DBA/2J retinas (Fig. 9E-F), the OPL was disrupted with a marked reduction of VGLUT1 immunoreactive axonal terminals and loss of calbindin immunoreactive horizontal cell processes (Fig. 9E, arrows; Fig. 9E, inset). In regions of the OPL that did not overlie the patches of inner retina with RGC loss, the giant mitochondrion were displaced to the ONL, whereas in ONL regions overlying the patches lacking RGCs, the number of giant mitochondrion decreased, likely due to the reduction of the number of photoreceptors. Furthermore, in OPL regions overlying the inner retina patches lacking RGCs, rod spherules had smaller appearance than those in the C57BL/6J control retinas and the horizontal cell endings, based on calbindin immunostaining and the giant mitochondria, based on Cyt C immunostaining were not observed (Fig. 9F, inset).

## DISCUSSION

Functional studies performed with glaucoma patients [40,41], and on glaucoma experimental animal models [42] and genetic models [13,15,43] showed that the a- and b-waves of the ERG were diminished compared to normal, age matched controls.

Findings from the present study also show outer retina pathology in the DBA/2J model in addition to their well-established loss of RGCs and axons. Altered ERGs are also correlated with outer retinal damage in a model of acute ocular hypertension [42], and recently, rod photoreceptor synaptic contacts have been reported to be reduced with aging [18]. The morphological changes described in this work could underlie the altered ERG responses observed in the DBA/2J mouse retina reported by other authors [13,15].

Photoreceptor and ON bipolar cells [16,17] mainly mediate the a- and b-waves of the ERG response. In this study, we performed an exhaustive characterization of the outer retina using immunohistochemical techniques with cellular markers for photoreceptor, bipolar and horizontal cells, before and after an increase in IOP in the DBA/2J mouse line. In general, IOP in this line begins to increase around 6 months of age [11,44]. In the DBA/2J line, alterations in the ONL and OPL were first observed at 3 months of age, before the increase of IOP. At this age, there was a diminution of photoreceptor cell bodies and OPL thickness, as well as a reduction in the occurrence of both pre and postsynaptic markers. The present study is in contrast to two earlier findings that the outer retina is unchanged in the DBA/2J mouse retina following the development of ocular pathology [10,29].

In the DBA/2J retina at all ages, there are changes in the connectivity of photoreceptor cells and their post-synaptic contacts, shown by a reduction in their connections with bipolar cell dendrites and horizontal cell processes. In addition, we have found retraction of bipolar and horizontal cell processes and a disruption of the photoreceptor

synaptic triad. Interestingly, in the 8 and 16 month old DBA/2J retinas, some horizontal and bipolar cell processes were located in the ONL, suggesting their growth was concomitant with outer retinal degeneration; interestingly, at 3 months of age bipolar and horizontal cell processes were shorter, suggesting a retraction of their processes. These results disagree with Fuchs and cols[18] findings. They described no alteration in horizontal and bipolar cells and attributed the thinning of the OPL to structural changes in rod synaptic ribbon but not cone photoreceptors[18]. We have carefully evaluated the pre and post-synaptic elements of the synaptic contacts in the OPL showing the loss of bipolar and horizontal cell dendrites and axons.

The growth of bipolar cells dendrites into the overlying ONL is a common feature in animal models of photoreceptor degeneration, including rd mice[45–47], the Royal College of Surgeons rats (RCS)[48] and P23H rats[27].

There are only a few functional and morphological studies of young DBA/2J mouse retinas; smaller amplitudes of the 2nd harmonic component of the flicker responses are noted at 2-3 month old compared to those registered in wild type animals, which could be due to the disruption of the synaptic triad in the photoreceptor terminals[13]. Furthermore, alterations in RIBEYE staining in rod photoreceptor ribbons were detected at 2 months old[18]. These findings are consistent with the idea that the Tyrp1 mutation that DBA/2J mice carry is expressed in the RPE[49], which may indirectly affect photoreceptor cells, since the health of the RPE is essential for the integrity of photoreceptors and normal retinal function[50]. For instance, in the adult retina, mutations altering the function of RPE lead to photoreceptor death[48,51].

With aging and IOP increased, the morphological changes in the OPL become quite prominent. In regions of the outer retina inside patches cellular degeneration is accelerated compared to other retinal regions. Moreover, at 16 months of age, the photoreceptor triad is disrupted and apparently absent in most cases, and the

horizontal cell plexus is absent. These morphological alterations in the OPL have been also described in an animal model of experimentally-induced increase of IOP[42].

Using double and triple immunostaining with markers for the synaptic ribbon, photoreceptor terminal, as well as for bipolar and horizontal cell processes, we studied the organization of the synaptic ribbon in the DBA/2J model. A decrease in photoreceptor ribbons with increased age was observed in the DBA/2J retina, based on the loss of Bassoon and CtBP2 immunoreactivity. Furthermore, we showed that although some photoreceptor axons expressed CtBP2, there was an absence of VGLUT1 immunoreactivity in the same terminals, suggesting that synaptic release of glutamate is greatly diminished or absent in the OPL[52] which is essential for visual information transmission[53]. These findings, together with the decoupling between photoreceptor terminals, bipolar cell dendrites and horizontal cell processes revealed by the loss of PKC and syntaxin 4 immunoreactivity, respectively, adjacent to synaptic ribbon markers is indicative of an impairment of the rod and cone synaptic structure.

Overall, these findings indicate a reduction in outer retinal signaling between photoreceptors, and bipolar cell dendrites and horizontal cell processes. This suggestion is consistent with a reduced ERG b-wave[54] in the Bassoon knockout mouse, which is characterized by a severely disrupted photoreceptor triad.

There are several different possibilities to account for the outer retinal pathology we observed in the DBA/2J retina:

First, outer retina impairment might be related to mutations of RPE genes and not to elevated IOP since the Tyrp1 gene is expressed by the RPE, at least at the initial stages of outer retinal degeneration. RPE dysfunction is a well-established cellular mechanism for photoreceptor and outer retinal diseases. RCS is a good example of a

retinitis pigmentosa animal model carrying a mutation in a RPE gene[55]. Mutations in Tyrp1 gene have been related to the etiology of human Oculocutaneous albinism type 3 (OPA3). Moreover, mutations in this gene generate endoplasmic reticulum (ER) stress due to misfolded protein accumulation[56], which could drive to RPE alterations. In addition, it has been shown that number of rod-photoreceptors is closely related to melanin levels in the RPE[57] and the fact that photoreceptors from albino animals are more susceptible to light damage[58,59] suggests the basis for outer retinal degeneration in DBA/2J mice.

Second, the increase of the IOP could result in two independent events; A) RGC and axonal damage that lead to RGC death, and B) photoreceptor cell damage that leads to outer retinal degeneration. This possibility cannot account for the changes in the outer retina that occur in young DBA/2J mice, before an increase of IOP.

Lastly, the mutations that the DBA/2J mice carry lead to ocular pathology typical of glaucoma before IOP increase, suggesting that this mouse glaucoma model is an IOP-independent glaucoma model. This suggestion is also based on findings that the DBA/2J model has two episodes of RGC loss[10], one occurs before the increase of IOP and is mainly mediated by apoptosis, and the second occurs after an increase IOP and is mainly mediated by necrosis. These observations are consistent with the early alterations in the outer and inner retina during an IOP-independent component followed by a component with increased IOP.

REFERENCES:


1. Quigley H a. Ganglion cell death in glaucoma: pathology recapitulates ontogeny. *Aust N Z J Ophthalmol*. 1995;23(2):85–91. Available at: http://www.ncbi.nlm.nih.gov/pubmed/7546696.
2. Quigley H a. Neuronal death in glaucoma. *Prog Retin Eye Res*. 1999;18(1):39–57. Available at: http://www.ncbi.nlm.nih.gov/pubmed/21255129.
3. Organization WH. Global data on visual impairments 2010. *URL http//www who int/blindness/ …*. 2012. Available at: http://scholar.google.com/scholar?hl=en&btnG=Search&q=intitle:Global+data+on+visual+impairments+2010#5. Accessed December 4, 2013.
4. Libby RT, Anderson MG, Pang I-H, et al. Inherited glaucoma in DBA/2J mice: pertinent disease features for studying the neurodegeneration. *Vis Neurosci*. 2005;22(5):637–48. doi:10.1017/S0952523805225130.
5. Schlamp CL, Li Y, Dietz J a, Janssen KT, Nickells RW. Progressive ganglion cell loss and optic nerve degeneration in DBA/2J mice is variable and asymmetric. *BMC Neurosci*. 2006;7:66. doi:10.1186/1471-2202-7-66.
6. Steele MR, Inman DM, Calkins DJ, Horner PJ, Vetter ML. Microarray analysis of retinal gene expression in the DBA/2J model of glaucoma. *Invest Ophthalmol Vis Sci*. 2006;47(3):977–85. doi:10.1167/iovs.05-0865.
7. Niyadurupola N, Broadway DC. Pigment dispersion syndrome and pigmentary glaucoma-a major review. *Clin Experiment Ophthalmol*. 2008;36(9):868–82. doi:10.1111/j.1442-9071.2009.01920.x.
8. Chang B, Smith R. Interacting loci cause severe iris atrophy and glaucoma in DBA / 2J mice. *Nat Genet*. 1999;21(april):405–409. Available at: http://scholar.google.com/scholar?hl=en&btnG=Search&q=intitle:Interacting+loci+cause+severe+iris+atrophy+and+glaucoma+in+DBA+/+2J+mice#0. Accessed September 26, 2012.
9. Anderson MG, Smith RS, Hawes NL, et al. Mutations in genes encoding melanosomal proteins cause pigmentary glaucoma in DBA/2J mice. *Nat Genet*. 2002;30(1):81–5. doi:10.1038/ng794.
10. Schuettauf F, Rejdak R, Walski M, et al. Retinal neurodegeneration in the DBA/2J mouse-a model for ocular hypertension. *Acta Neuropathol*. 2004;107(4):352–8. doi:10.1007/s00401-003-0816-9.
11. John SW, Smith RS, Savinova O V, et al. Essential iris atrophy, pigment dispersion, and glaucoma in DBA/2J mice. *Invest Ophthalmol Vis Sci*. 1998;39(6):951–62. Available at: http://www.ncbi.nlm.nih.gov/pubmed/9579474.
12. Raymond ID, Pool AL, Vila A, Brecha NC. A Thy1-CFP DBA/2J mouse line with cyan fluorescent protein expression in retinal ganglion cells. *Vis Neurosci*. 2009;26(5-6):453–65. doi:10.1017/S095252380999023X.
13. Harazny J, Scholz M, Buder T, Lausen B, Kremers J. Electrophysiological deficits in the retina of the DBA/2J mouse. *Doc Ophthalmol*. 2009;119(3):181–97. doi:10.1007/s10633-009-9194-5.
14. Barabas P, Huang W, Chen H, et al. Missing optomotor head-turning reflex in the DBA/2J mouse. *Invest Ophthalmol Vis Sci*. 2011;52(9):6766–73. doi:10.1167/iovs.10-7147.
15. Heiduschka P, Julien S, Schuettauf F, Schnichels S. Loss of retinal function in aged DBA/2J mice - New insights into retinal neurodegeneration. *Exp Eye Res*. 2010;91(5):779–83. doi:10.1016/j.exer.2010.09.001.
16. Brown K, Wiesel T. Localization of origins of electroretinogram components by intraretinal recording in the intact cat eye. *J Physiol*. 1961:257–280. Available at: http://jp.physoc.org/content/158/2/257.full.pdf. Accessed September 26, 2012.
17. Tomita T. Electrical activity of vertebrate photoreceptors. *Nihon Seirigaku Zasshi*. 1970;32(8):567–8. Available at: http://www.ncbi.nlm.nih.gov/pubmed/5530093.

18. Fuchs M, Scholz M, Sendelbeck A, et al. Rod photoreceptor ribbon synapses in DBA/2J mice show progressive age-related structural changes. *PLoS One*. 2012;7(9):e44645. doi:10.1371/journal.pone.0044645.
19. Fernández-Sánchez L, Lax P, Pinilla I, Martín-Nieto J, Cuenca N. Tauroursodeoxycholic acid prevents retinal degeneration in transgenic P23H rats. *Invest Ophthalmol Vis Sci*. 2011;52(8):4998–5008. doi:10.1167/iovs.11-7496.
20. Fernández-Sánchez L, Lax P, Esquiva G, Martín-Nieto J, Pinilla I, Cuenca N. Safranal, a saffron constituent, attenuates retinal degeneration in P23H rats. *PLoS One*. 2012;7(8):e43074. doi:10.1371/journal.pone.0043074.
21. Rodriguez-de la Rosa L, Fernandez-Sanchez L, Germain F, et al. Age-related functional and structural retinal modifications in the Igf1-/- null mouse. *Neurobiol Dis*. 2012;46(2):476–85. doi:10.1016/j.nbd.2012.02.013.
22. Martinez-Navarrete G, Seiler MJ, Aramant RB, Fernandez-Sanchez L, Pinilla I, Cuenca N. Retinal degeneration in two lines of transgenic S334ter rats. *Exp Eye Res*. 2011;92(3):227–37. doi:10.1016/j.exer.2010.12.001.
23. Dowling JE, Chappell RL. Neural organization of the median ocellus of the dragonfly. II. Synaptic structure. *J Gen Physiol*. 1972;60(2):148–65. Available at: http://www.pubmedcentral.nih.gov/articlerender.fcgi?artid=2226068&tool=pmcentrez&rendertype=abstract.
24. Kolb H, Nelson R, Ahnelt P, Cuenca N. Cellular organization of the vertebrate retina. *Prog Brain Res*. 2001;131:3–26. Available at: http://www.sciencedirect.com/science/article/pii/S0079612301310051. Accessed September 26, 2012.
25. Linberg K, Cuenca N, Ahnelt P, Fisher S, Kolb H. Comparative anatomy of major retinal pathways in the eyes of nocturnal and diurnal mammals. *Prog Brain Res*. 2001;131:27–52. Available at: http://www.sciencedirect.com/science/article/pii/S0079612301310063. Accessed September 26, 2012.
26. Brandstätter JH, Fletcher EL, Garner CC, Gundelfinger ED, Wässle H. Differential expression of the presynaptic cytomatrix protein bassoon among ribbon synapses in the mammalian retina. *Eur J Neurosci*. 1999;11(10):3683–93. Available at: http://www.ncbi.nlm.nih.gov/pubmed/10564375.
27. Cuenca N, Pinilla I, Sauvé Y, Lu B, Wang S, Lund RD. Regressive and reactive changes in the connectivity patterns of rod and cone pathways of P23H transgenic rat retina. *Neuroscience*. 2004;127(2):301–17. doi:10.1016/j.neuroscience.2004.04.042.
28. Martínez-Navarrete GC, Martín-Nieto J, Esteve-Rudd J, Angulo A, Cuenca N. Alpha synuclein gene expression profile in the retina of vertebrates. *Mol Vis*. 2007;13(October 2006):949–61. Available at: http://www.pubmedcentral.nih.gov/articlerender.fcgi?artid=3380420&tool=pmcentrez&rendertype=abstract.
29. Jakobs TC, Libby RT, Ben Y, John SWM, Masland RH. Retinal ganglion cell degeneration is topological but not cell type specific in DBA/2J mice. *J Cell Biol*. 2005;171(2):313–25. doi:10.1083/jcb.200506099.
30. Peng Y-W, Senda T, Hao Y, Matsuno K, Wong F. Ectopic synaptogenesis during retinal degeneration in the royal college of surgeons rat. *Neuroscience*. 2003;119(3):813–820. doi:10.1016/S0306-4522(03)00153-2.
31. Ritchey ER, Bongini RE, Code K a, Zelinka C, Petersen-Jones S, Fischer a J. The pattern of expression of guanine nucleotide-binding protein beta3 in the retina is conserved across vertebrate species. *Neuroscience*. 2010;169(3):1376–91. doi:10.1016/j.neuroscience.2010.05.081.
32. Gong J, Jellali A, Mutterer J, Sahel J a, Rendon A, Picaud S. Distribution of vesicular glutamate transporters in rat and human retina. *Brain Res*. 2006;1082(1):73–85. doi:10.1016/j.brainres.2006.01.111.

33. Heidelberger R, Thoreson WB, Witkovsky P. Synaptic transmission at retinal ribbon synapses. *Prog Retin Eye Res*. 2005;24(6):682–720. doi:10.1016/j.preteyeres.2005.04.002.
34. tom Dieck S, Altrock WD, Kessels MM, et al. Molecular dissection of the photoreceptor ribbon synapse: physical interaction of Bassoon and RIBEYE is essential for the assembly of the ribbon complex. *J Cell Biol*. 2005;168(5):825–36. doi:10.1083/jcb.200408157.
35. Schmitz F, Ko A, Su TC, Molekularbiologie AN. RIBEYE , a Component of Synaptic Ribbons : A Protein ' s Journey through Evolution Provides Insight into Synaptic Ribbon Function. 2000;28:857–872.
36. Hirano A, Brandstatter J, Vila A, Brecha N. Robust syntaxin-4 immunoreactivity in mammalian horizontal cell processes. *Vis Neurosci*. 2007;24(4):489–502. doi:10.1017/S0952523807070198.Robust.
37. Medrano CJ, Fox D a. Oxygen consumption in the rat outer and inner retina: light- and pharmacologically-induced inhibition. *Exp Eye Res*. 1995;61(3):273–84. Available at: http://www.ncbi.nlm.nih.gov/pubmed/7556491.
38. Heidelberger R. Roles of ATP in Depletion and Replenishment of the Releasable Pool of Synaptic Vesicles. *J Neurophysiol*. 2002:98–106. Available at: http://jn.physiology.org/content/88/1/98.short. Accessed September 26, 2012.
39. Johnson JE, Perkins G a, Giddabasappa A, et al. Spatiotemporal regulation of ATP and Ca2+ dynamics in vertebrate rod and cone ribbon synapses. *Mol Vis*. 2007;13(February):887–919. Available at: http://www.pubmedcentral.nih.gov/articlerender.fcgi?artid=2774461&tool=pmcentrez&rendertype=abstract.
40. Korth M, Nguyen NX, Horn F, Martus P. Scotopic threshold response and scotopic PII in glaucoma. *Invest Ophthalmol Vis Sci*. 1994;35(2):619–25. Available at: http://www.ncbi.nlm.nih.gov/pubmed/8113012.
41. Vaegan, Graham SL, Goldberg I, Buckland L, Hollows FC. Flash and pattern electroretinogram changes with optic atrophy and glaucoma. *Exp Eye Res*. 1995;60(6):697–706. Available at: http://www.ncbi.nlm.nih.gov/pubmed/7641852.
42. Cuenca N, Pinilla I, Fernández-Sánchez L, et al. Changes in the inner and outer retinal layers after acute increase of the intraocular pressure in adult albino Swiss mice. *Exp Eye Res*. 2010;91(2):273–85. doi:10.1016/j.exer.2010.05.020.
43. Bayer AU, Neuhardt T, May AC, et al. Retinal Morphology and ERG Response in the DBA / 2NNia Mouse Model of Angle-Closure Glaucoma. 2001;42(6):1258–1265.
44. Saleh M, Nagaraju M, Porciatti V. Longitudinal evaluation of retinal ganglion cell function and IOP in the DBA/2J mouse model of glaucoma. *Invest Ophthalmol Vis Sci*. 2007;48(10):4564–72. doi:10.1167/iovs.07-0483.
45. Rossi C, Strettoi E, Galli-Resta L. The spatial order of horizontal cells is not affected by massive alterations in the organization of other retinal cells. *J Neurosci*. 2003;23(30):9924–8. Available at: http://www.ncbi.nlm.nih.gov/pubmed/14586022.
46. Strettoi E, Pignatelli V. Modifications of retinal neurons in a mouse model of retinitis pigmentosa. *Proc Natl Acad Sci U S A*. 2000;97(20):11020–5. doi:10.1073/pnas.190291097.
47. Strettoi E, Pignatelli V, Rossi C, Porciatti V, Falsini B. Remodeling of second-order neurons in the retina of rd/rd mutant mice. *Vision Res*. 2003;43(8):867–877. doi:10.1016/S0042-6989(02)00594-1.
48. Cuenca N, Pinilla I, Sauve Y, Lund R. Early changes in synaptic connectivity following progressive photoreceptor degeneration in RCS rats. 2005;22(March):1057–1072. doi:10.1111/j.1460-9568.2005.04300.x.
49. Mori M, Metzger D, Garnier J-M, Chambon P, Mark M. Site-specific somatic mutagenesis in the retinal pigment epithelium. *Invest Ophthalmol Vis Sci*.

2002;43(5):1384–8. Available at:
http://www.ncbi.nlm.nih.gov/pubmed/11980850.
50. Raymond SM, Jackson IJ. The retinal pigmented epithelium is required for development and maintenance of the mouse neural retina. *Curr Biol*. 1995;5(11):1286–95. Available at:
http://www.ncbi.nlm.nih.gov/pubmed/8574586.
51. Pinilla I, Cuenca N, Sauvé Y, Wang S, Lund RD. Preservation of outer retina and its synaptic connectivity following subretinal injections of human RPE cells in the Royal College of Surgeons rat. *Exp Eye Res*. 2007;85(3):381–92. doi:10.1016/j.exer.2007.06.002.
52. Schuettauf F, Thaler S, Bolz S, et al. Alterations of amino acids and glutamate transport in the DBA/2J mouse retina; possible clues to degeneration. *Graefes Arch Clin Exp Ophthalmol*. 2007;245(8):1157–68. doi:10.1007/s00417-006-0531-z.
53. Johnson J, Fremeau RT, Duncan JL, et al. Vesicular glutamate transporter 1 is required for photoreceptor synaptic signaling but not for intrinsic visual functions. *J Neurosci*. 2007;27(27):7245–55. doi:10.1523/JNEUROSCI.0815-07.2007.
54. Dick O, tom Dieck S, Altrock WD, et al. The presynaptic active zone protein bassoon is essential for photoreceptor ribbon synapse formation in the retina. *Neuron*. 2003;37(5):775–86. Available at:
http://www.ncbi.nlm.nih.gov/pubmed/12628168.
55. D'Cruz PM, Yasumura D, Weir J, et al. Mutation of the receptor tyrosine kinase gene Mertk in the retinal dystrophic RCS rat. *Hum Mol Genet*. 2000;9(4):645–51. Available at: http://www.ncbi.nlm.nih.gov/pubmed/10699188.
56. Toyofuku K, Wada I, Valencia JC, Kushimoto T, Ferrans VJ, Hearing VJ. Oculocutaneous albinism types 1 and 3 are ER retention diseases: mutation of tyrosinase or Tyrp1 can affect the processing of both mutant and wild-type proteins. *FASEB J*. 2001;15(12):2149–61. doi:10.1096/fj.01-0216com.
57. Donatien P, Jeffery G. Correlation between Rod Photoreceptor Numbers and Levels of Ocular Pigmentation. 2002:1198–1203.
58. Sanyal S, Zeilmaker GH. Retinal damage by constant light in chimaeric mice: implications for the protective role of melanin. Exp Eye Res. 1988;46(5):731-43. PubMed PMID: 3384019.
59. Jansen HG, Sanyal S. Synaptic changes in the terminals of rod photoreceptors of albino mice after partial visual cell loss induced by brief exposure to constant light. Cell Tissue Res. 1987;250(1):43-52. PubMed PMID: 3652165.
60. Barhoum R, Martínez-Navarrete G, Corrochano S, et al. Functional and structural modifications during retinal degeneration in the rd10 mouse. *Neuroscience*. 2008;155(3):698–713. doi:10.1016/j.neuroscience.2008.06.042.
61. Rossé T, Olivier R, Monney L, et al. Bcl-2prolongscell survival afterBax-induced releaseofcytochromec. 1998;391(January):1–4.
62. Zhang H, Li S, Doan T, et al. Deletion of PrBP/delta impedes transport of GRK1 and PDE6 catalytic subunits to photoreceptor outer segments. *Proc Natl Acad Sci U S A*. 2007;104(21):8857–62. doi:10.1073/pnas.0701681104.

FIGURE LEGENDS:

**Figure 1.** Vertical sections from C57BL/6J retina at 16 months (A), and DBA/2J retina at 3, 8 and 16 months (B-D). Immunostained with the nuclear marker TO-PRO 3-iodide showed a reduction in the number of cellular rows in the ONL and INL and a reduction in cell bodies in the GCL, likely corresponding to RGCs. The quantification is shown in E (**$p < 0.01$). ONL: outer nuclear layer; OPL: outer plexiform layer; INL: inner nuclear layer; IPL: inner plexiform layer; GCL: ganglion cell layer. Scale bar: 20 μm.

**Figure 2.** Immunolabeling for α-PKC (green) and Bassoon (red) on vertical sections. (A-C) C57BL/6J retina at 16 months of age. DBA/2J retina at 3 months (D-F), 8 months (G-I) and 16 months (J-L). (A, D, G, J): Immunolabeling for α-PKC showing loss of dendrites of rod bipolar cells in the DBA/2J retina in older animals. (B, E, H, K): Immunolabeling for Bassoon showing the diminution of synaptic ribbons in the OPL in this animal model. (C, L, F, I) Merge. ONL: outer nuclear layer; OPL: outer plexiform layer; INL: inner nuclear layer. Scale bar: 10 μm.

**Figure 3.** Cryostat sections of C57BL/6J (A-C) and DBA/2J retinas at 3 months (D-F), 8 months (G-I) and 16 months (J-L). Immunolabeling for calbindin (A, D, G, J; arrowheads) showing the loss of terminal tips of horizontal cells in the DBA/2J retina. Immunolabeling for synaptophysin (B, E, H, K) showing the diminution of the photoreceptor axon terminals. (C, L, F, I) Merge. ONL: outer nuclear layer; OPL: outer plexiform layer; INL: inner nuclear layer. Scale bar: 10 μm.

**Figure 4.** Low magnification cross section of retinas labeled with antibodies against α-PKC (red), calbindin (green) and VGLUT1 (blue). DBA/2J retina at 16 months old (A) showing a

panoramic view of a retinal patch (area underlying white line). In high magnification of this area (C: high magnification from C') the loss of photoreceptor cells, sprouting of bipolar and horizontal cells into the ONL (arrowheads), loss of horizontal plexus in the OPL and vascular alterations (arrows) can be observed compared to areas outside patches (B, D: high magnification from B' and D' in A, respectively). ONL: outer nuclear layer, INL: inner nuclear layer, GCL: ganglion cell layer. Scale bar: (A) 200 μm; (B-D) 40 μm.

**Figure 5.** Retinal morphology of cone photoreceptor. γ-transducin antibodies were used to visualize cone morphology in vertical retina sections of C57BL/6 retinas (A), DBA/2J retinas at 3 months (B), 8 months (C, D) and 16 months (E, F). The nuclei of cone photoreceptor showed an abnormal localization at the ONL level at 3 months (B, arrow) and at 16 months (E, arrow). Inside the patches (D, F) the IS of cones were swollen (arrowheads) and had short axons or absents (double arrowheads). OS: outer segments; IS: inner segments; ONL: outer nuclear layer; OPL: outer plexiform layer; INL: inner nuclear layer; IPL: inner plexiform layer. Scale bar: 20 μm.

**Figure 6.** Bipolar cells immunostained with GNB3 antibodies. The GNB3 staining showed retraction of bipolar dendrites at 3 months old in the DBA/2J retina (B, arrowheads) compared with C57BL/6 retina (A). DBA/2J retinas have bipolar cell dendritic growth at 8 months (C, D, arrows) until 16 months of age (E, arrows; F). This dendritic growth was more evident inside the patches (D, F). ONL: outer nuclear layer; OPL: outer plexiform layer; INL: inner nuclear layer; IPL: inner plexiform layer. Scale bar: 20 μm.

**Figure 7.** Three specific markers of synaptic structure were used to study the connectivity between photoreceptor and horizontal cells. Antibodies against CtBP2 (red) and VGLUT1 (blue) were used to visualize the axon terminal structures of photoreceptor cells, and calbindin (green) were used to visualize horizontal cell dendrites. A thinning in the OPL was

observed at 3 months old in the DBA/2J retinas (B) compared with C57BL/6 retinas (A). From 8 months (C, D) to 16 months (E, F), DBA/2J retinas showed growth of horizontal cells and synaptic contacts without VGLUT1 immunoreactivity (arrowheads). At 16 months old, inside the patches, only some synaptic contacts were complete (F, arrows) and the plexus of the horizontal cells at OPL level were nearly absent. Quantification of horizontal cell terminal tips is shown in G (*$p < 0.05$). ONL: outer nuclear layer; OPL: outer plexiform layer; INL: inner nuclear layer. Scale bar: 10 μm.

**Figure 8.** Study of connectivity lost between photoreceptor and horizontal cells. A double immunostaining against syntaxin 4 (green) and CtBP2 (red) was used to evaluate the loss of photoreceptor and horizontal contacts. In the C57BL/6 retinas (A) and in DBA/2J retinas at 3 months old (B), each point of CtBP2 had the corresponding syntaxin 4 (STX4) spot. This relation was disrupted from 8 months old inside the patches (D, arrowheads) to 16 months old in the DBA/2J retinas (E, F, arrowheads). There was a reduction in the contacts at 8 months old in the DBA/2J retinas. OPL: outer plexiform layer. Scale bar: 10 μm.

**Figure 9.** Vertical sections of retinas stained with antibodies against calbindin (green) to visualize horizontal dendrite tips, VGLUT1 (red) for photoreceptor axon terminals staining and cytochrome C (blue) to visualize the giant mitochondria. The panel shows normal connections between photoreceptor and horizontal cells in C57BL/6 retinas at 16 months (A) compared with the connections of DBA/2J retinas at 3 months where some photoreceptor axons have lost VGLUT1 staining (B, arrows). At 8 months (C, D), DBA/2J retinas show growth of horizontal cell processes outside the patches (C, arrows) and loss of contacts with photoreceptor axons and horizontal tip retraction (C, arrowheads). DBA/2J retinas at 16 months of age have some axon terminals adjacent to horizontal cells processes both out and inside the patches (E, F; arrows). ONL: outer nuclear layer; OPL: outer plexiform layer; INL: inner nuclear layer. Scale bar: 10 μm. Scale bar in the high magnification: 2 μm.

**Supplementary materials:**

**Figure S1.** Retinal cross section labeled with antibodies against calbindin (green) and Synaptophysin (red). (A) 16 old month DBA/2J retina showing a panoramic view of a retinal patch (area underlying white line). (C) High magnification from C' showing loss of photoreceptor cells and loss of horizontal plexus in the OPL compared to high magnification areas outside patches (B, D: high magnification from B' and D', respectively). ONL: outer nuclear layer, INL: inner nuclear layer, GCL: ganglion cell layer. Scale bar: (A) 200 μm; (B-D) 40 μm.

**Figure S2.** Whole mount retina stained with antibodies against Brn3a to visualize RGC loss in C57BL/6 (A) and DBA/2J (B). DBA/2J whole mount retina at 16 months old (B) showing areas with loss of RGCs, surrounded by areas, in which still have surviving RGCs. Scale bar: 200 μm.

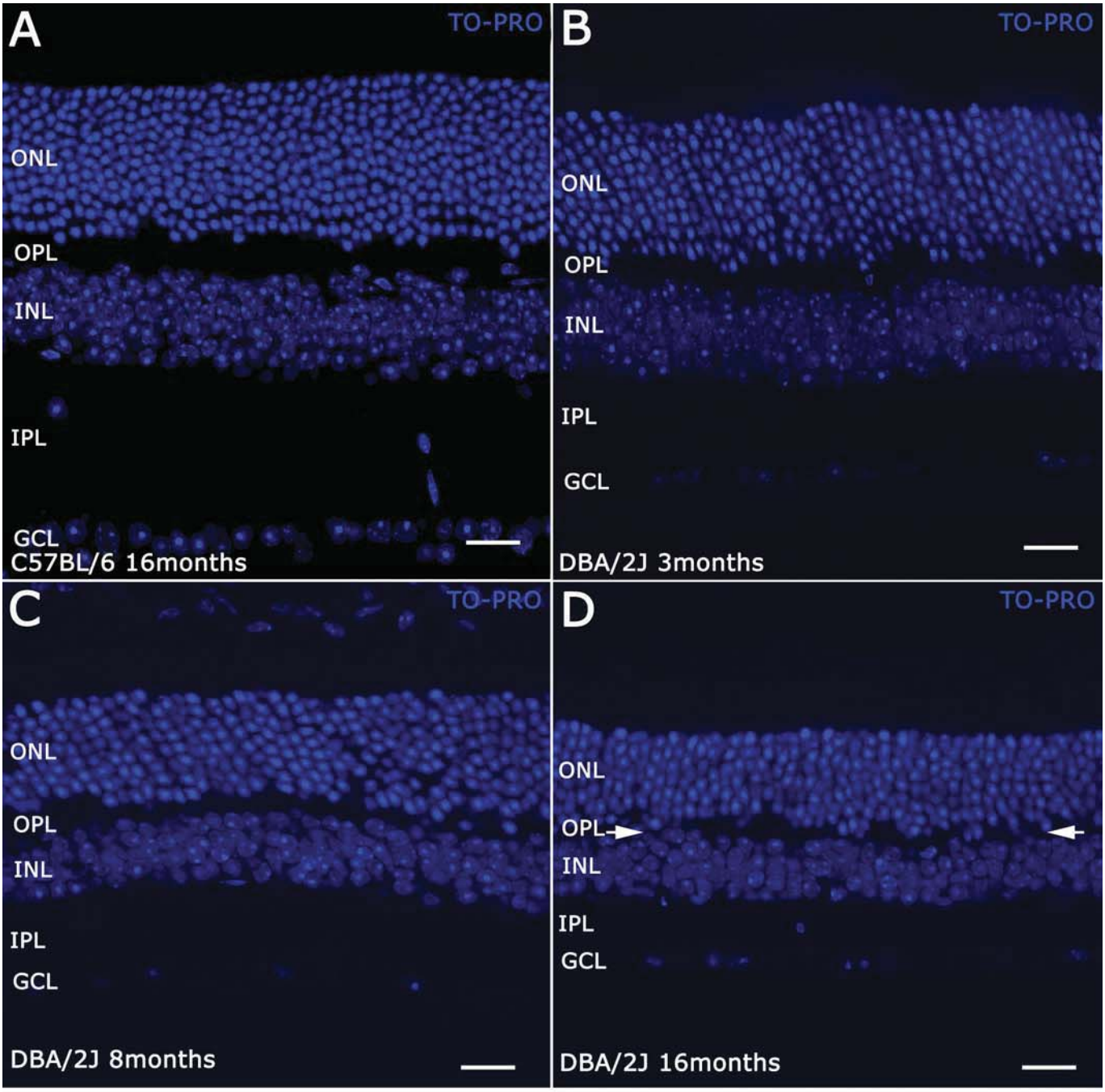
A
TO-PRO
ONL
OPL
INL
IPL
GCL
C57BL/6 16months
B
TO-PRO
ONL
OPL
INL
IPL
GCL
DBA/2J 3months
C
TO-PRO
ONL
OPL
INL
IPL
GCL
DBA/2J 8months
D
TO-PRO
ONL
OPL
INL
IPL
GCL
DBA/2J 16months

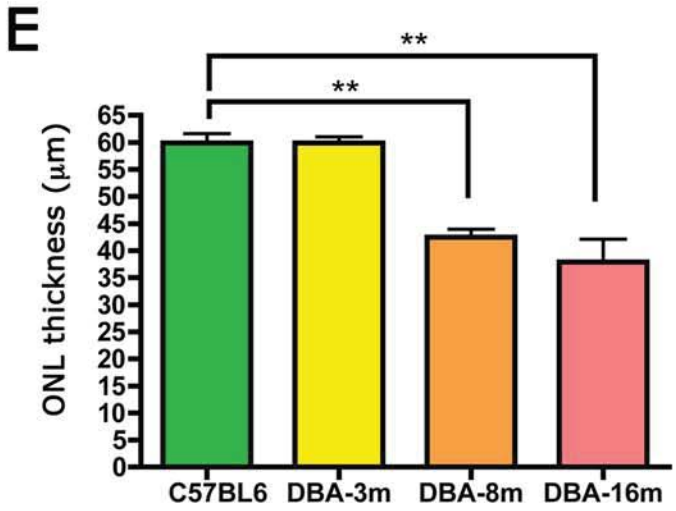
E
**
**
ONL thickness (µm)
65
60
55
50
45
40
35
30
25
20
15
10
5
0
C57BL6
DBA-3m
DBA-8m
DBA-16m

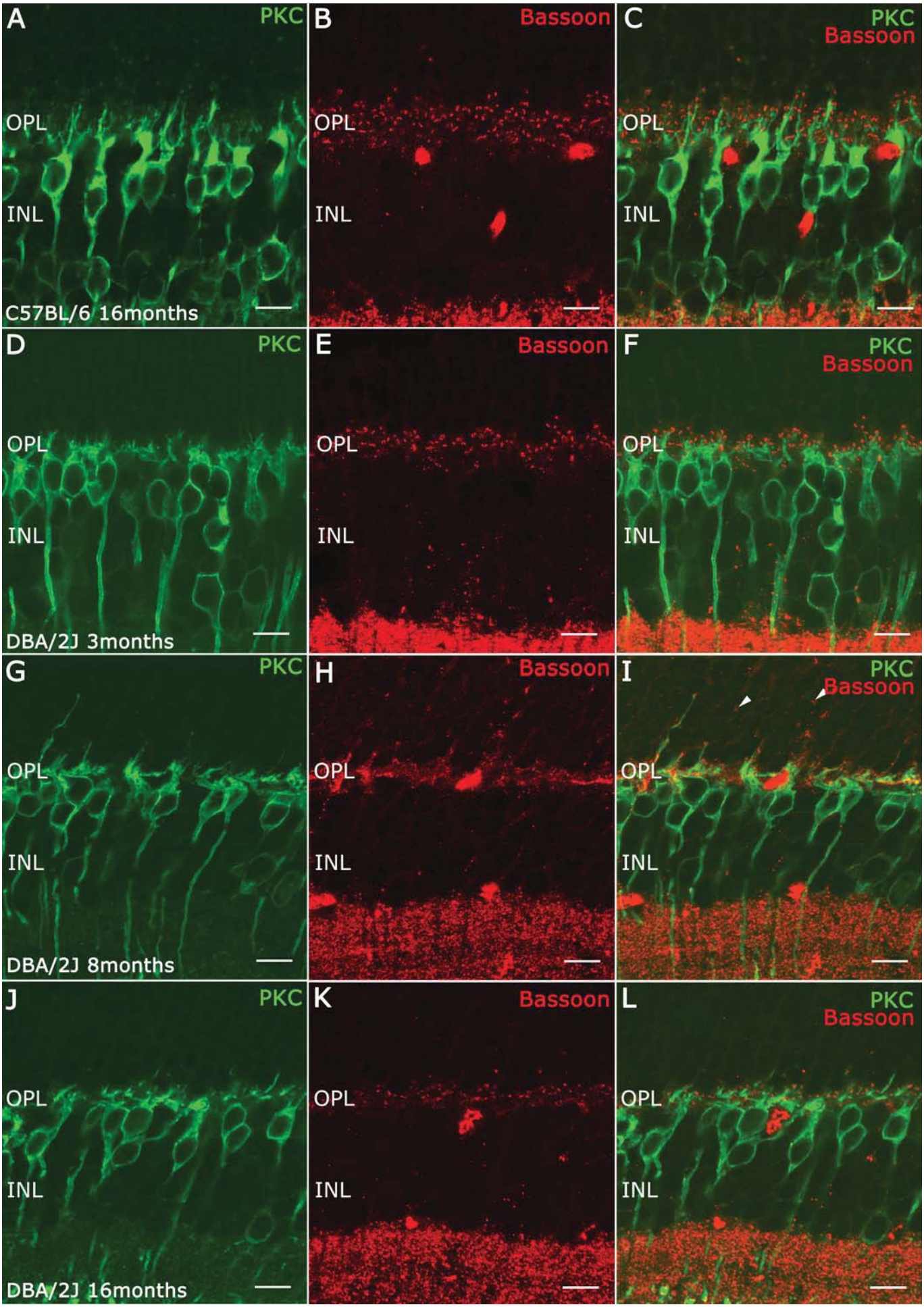
A
PKC
OPL
INL
C57BL/6 16months
B
Bassoon
OPL
INL
C
PKC
Bassoon
OPL
INL
D
PKC
OPL
INL
DBA/2J 3months
E
Bassoon
OPL
INL
F
PKC
Bassoon
OPL
INL
G
PKC
OPL
INL
DBA/2J 8months
H
Bassoon
OPL
INL
I
PKC
Bassoon
OPL
INL
J
PKC
OPL
INL
DBA/2J 16months
K
Bassoon
OPL
INL
L
PKC
Bassoon
OPL
INL

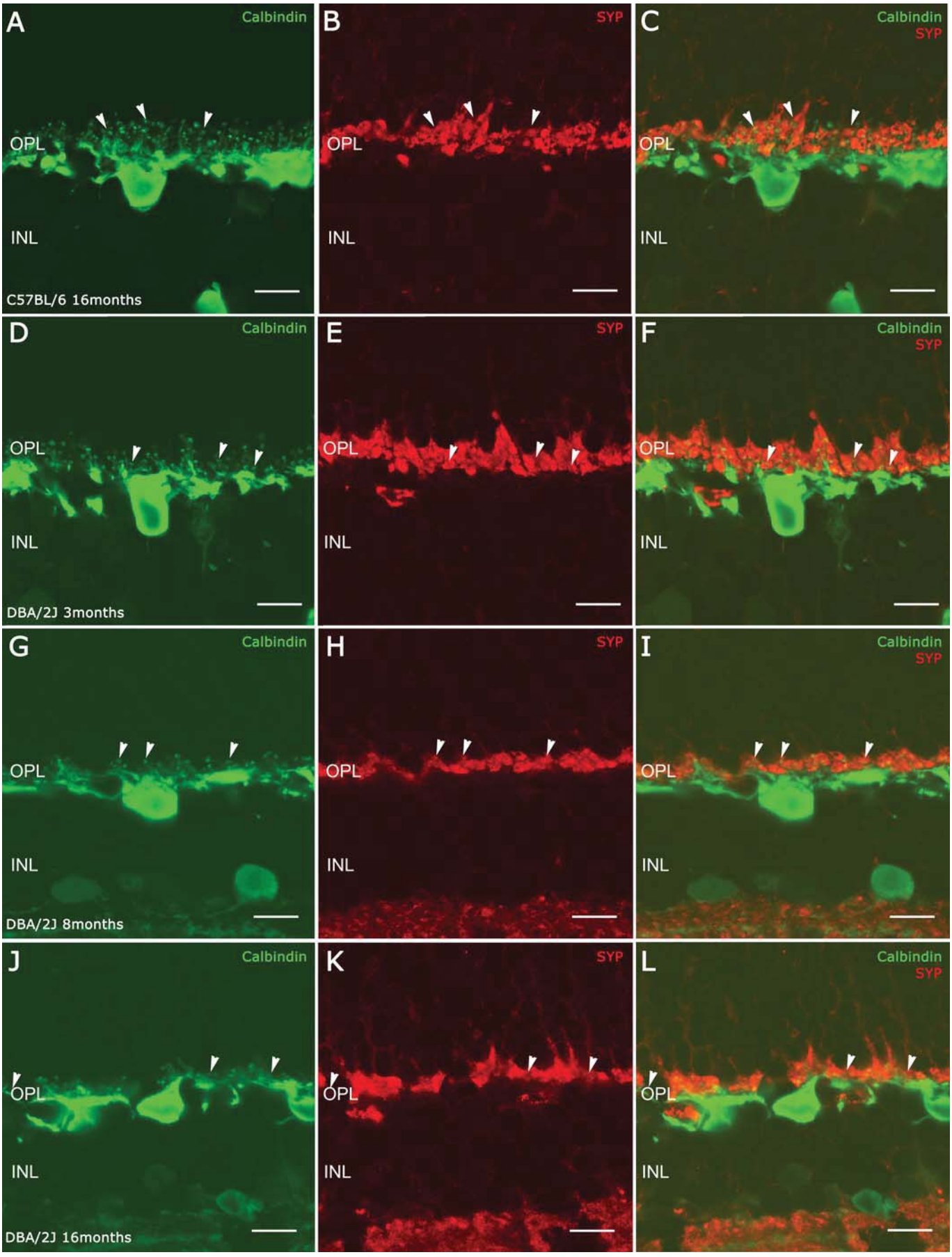
A
Calbindin
OPL
INL
C57BL/6 16months
B
SYP
OPL
INL
C
Calbindin
SYP
OPL
INL
D
Calbindin
OPL
INL
DBA/2J 3months
E
SYP
OPL
INL
F
Calbindin
SYP
OPL
INL
G
Calbindin
OPL
INL
DBA/2J 8months
H
SYP
OPL
INL
I
Calbindin
SYP
OPL
INL
J
Calbindin
OPL
INL
DBA/2J 16months
K
SYP
OPL
INL
L
Calbindin
SYP
OPL
INL

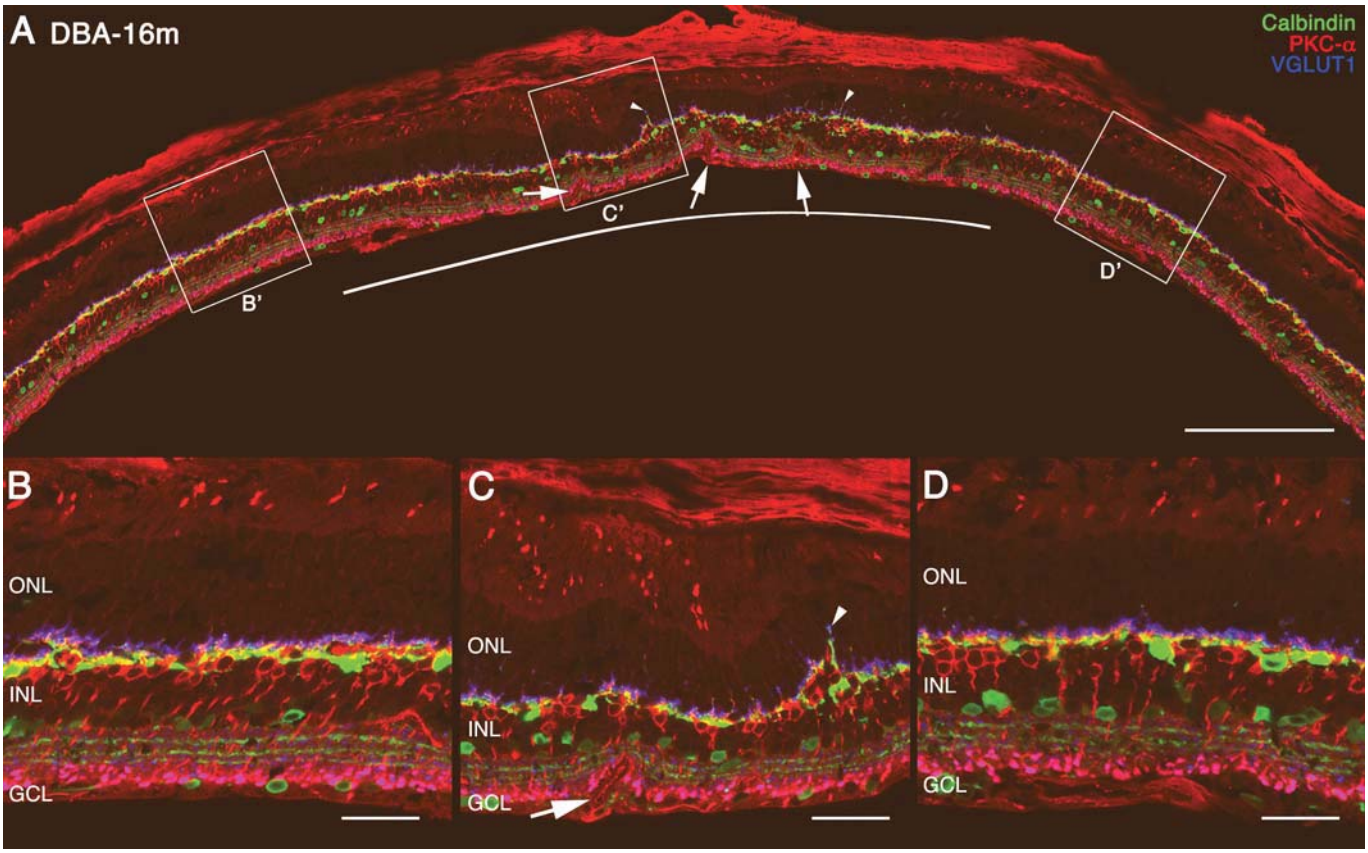
A DBA-16m
Calbindin
PKC-α
VGLUT1
B'
C'
D'
B
ONL
INL
GCL
C
ONL
INL
GCL
D
ONL
INL
GCL

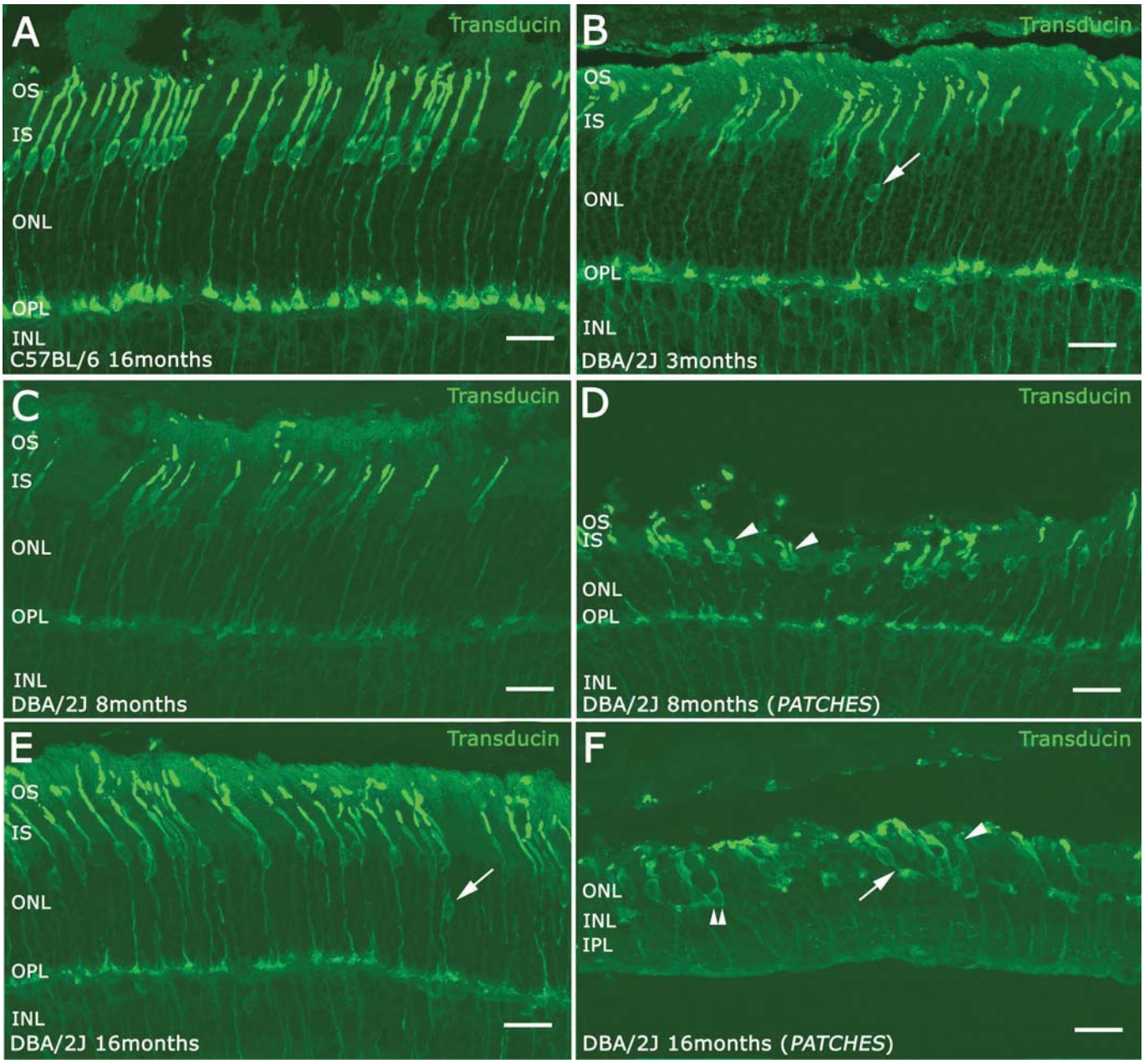
A
Transducin
OS
IS
ONL
OPL
INL
C57BL/6 16months
B
Transducin
OS
IS
ONL
OPL
INL
DBA/2J 3months
C
Transducin
OS
IS
ONL
OPL
INL
DBA/2J 8months
D
Transducin
OS
IS
ONL
OPL
INL
DBA/2J 8months (PATCHES)
E
Transducin
OS
IS
ONL
OPL
INL
DBA/2J 16months
F
Transducin
ONL
INL
IPL
DBA/2J 16months (PATCHES)

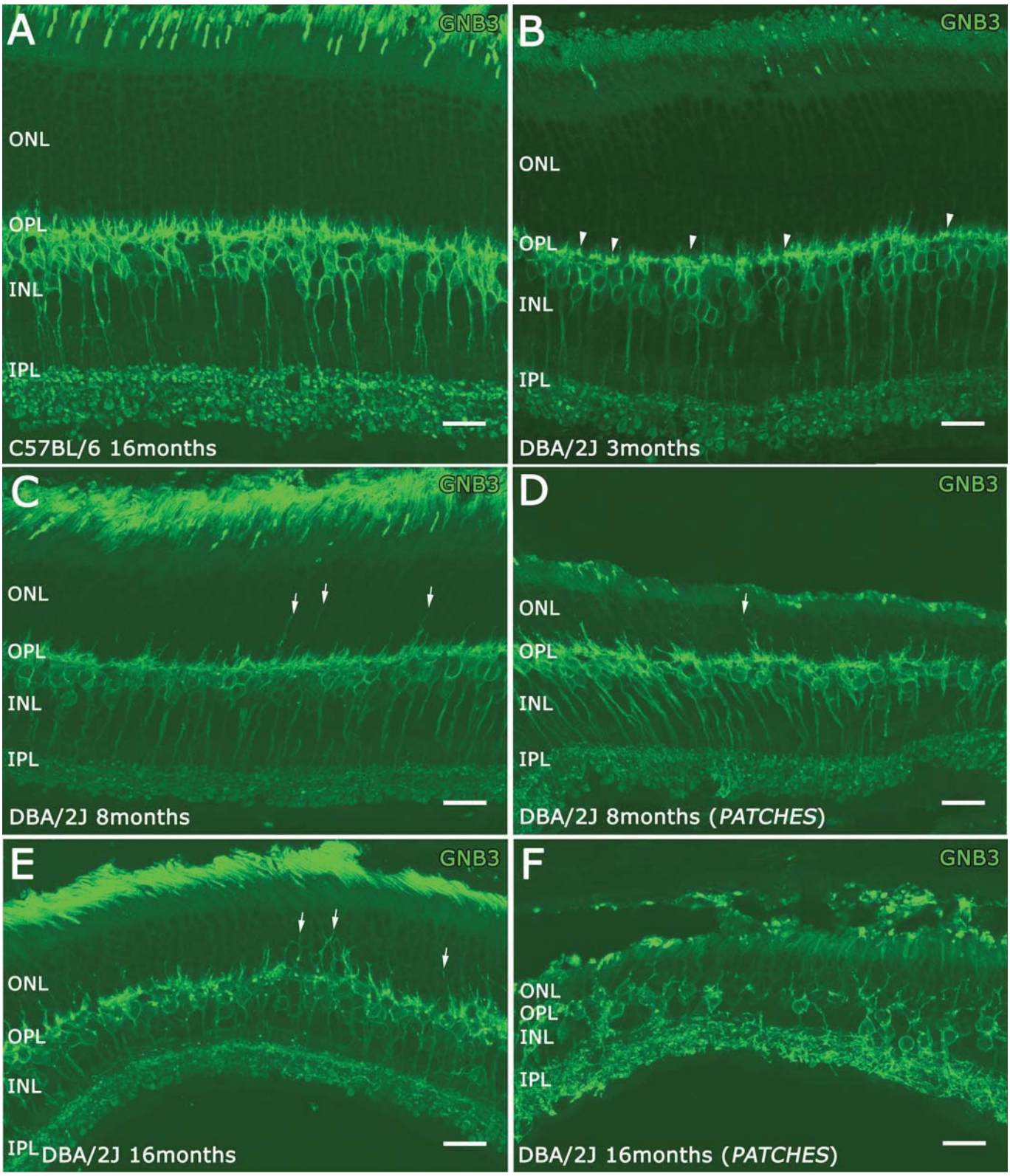
A
GNB3
ONL
OPL
INL
IPL
C57BL/6 16months
B
GNB3
ONL
OPL
INL
IPL
DBA/2J 3months
C
GNB3
ONL
OPL
INL
IPL
DBA/2J 8months
D
GNB3
ONL
OPL
INL
IPL
DBA/2J 8months (PATCHES)
E
GNB3
ONL
OPL
INL
IPL
DBA/2J 16months
F
GNB3
ONL
OPL
INL
IPL
DBA/2J 16months (PATCHES)

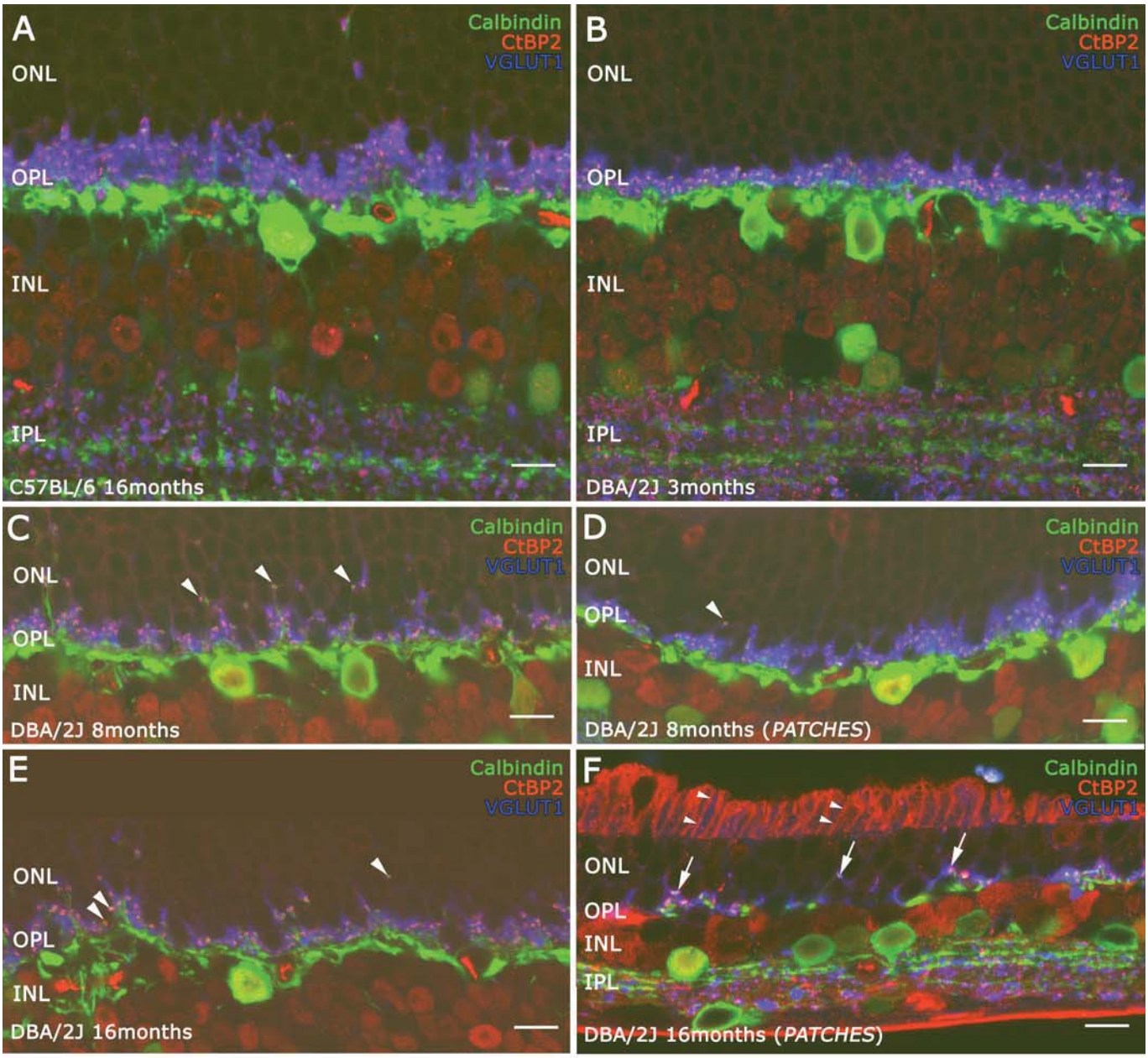
A
Calbindin
CtBP2
VGLUT1
ONL
OPL
INL
IPL
C57BL/6 16months
B
Calbindin
CtBP2
VGLUT1
ONL
OPL
INL
IPL
DBA/2J 3months
C
Calbindin
CtBP2
VGLUT1
ONL
OPL
INL
DBA/2J 8months
D
Calbindin
CtBP2
VGLUT1
ONL
OPL
INL
DBA/2J 8months (PATCHES)
E
Calbindin
CtBP2
VGLUT1
ONL
OPL
INL
DBA/2J 16months
F
Calbindin
CtBP2
VGLUT1
ONL
OPL
INL
IPL
DBA/2J 16months (PATCHES)

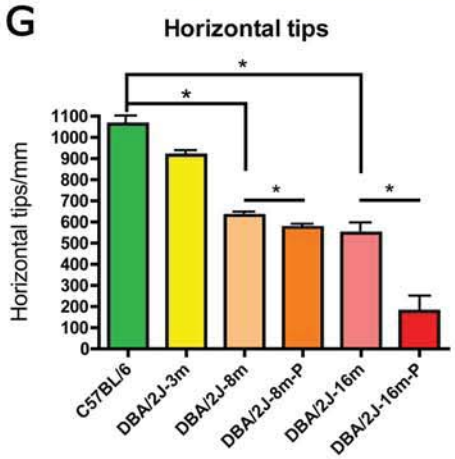
G
Horizontal tips
Horizontal tips/mm
1100
1000
900
800
700
600
500
400
300
200
100
0
*
*
*
*
C57BL/6
DBA/2J-3m
DBA/2J-8m
DBA/2J-8m-P
DBA/2J-16m
DBA/2J-16m-P

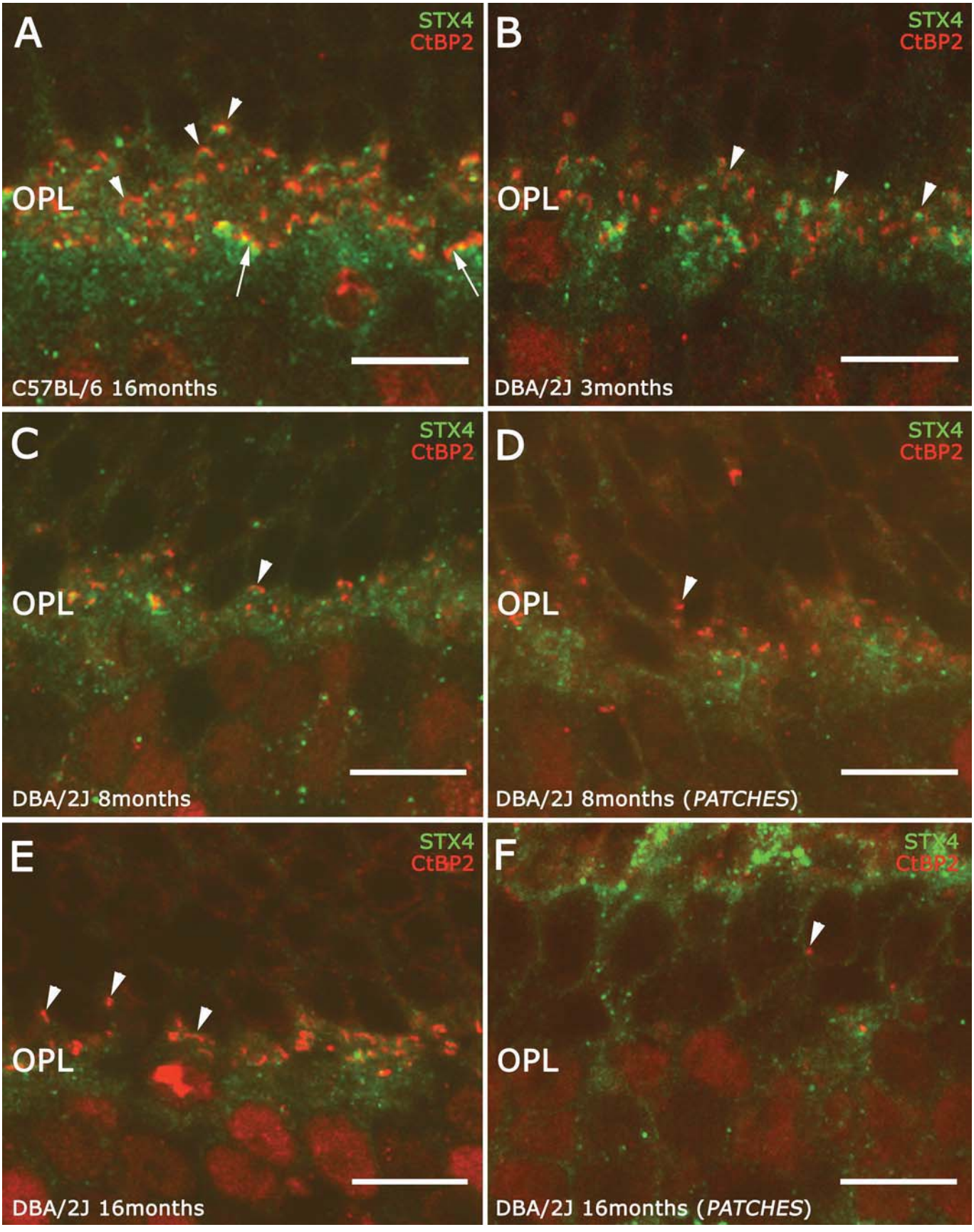
A
STX4
CtBP2
OPL
C57BL/6 16months
B
STX4
CtBP2
OPL
DBA/2J 3months
C
STX4
CtBP2
OPL
DBA/2J 8months
D
STX4
CtBP2
OPL
DBA/2J 8months (PATCHES)
E
STX4
CtBP2
OPL
DBA/2J 16months
F
STX4
CtBP2
OPL
DBA/2J 16months (PATCHES)

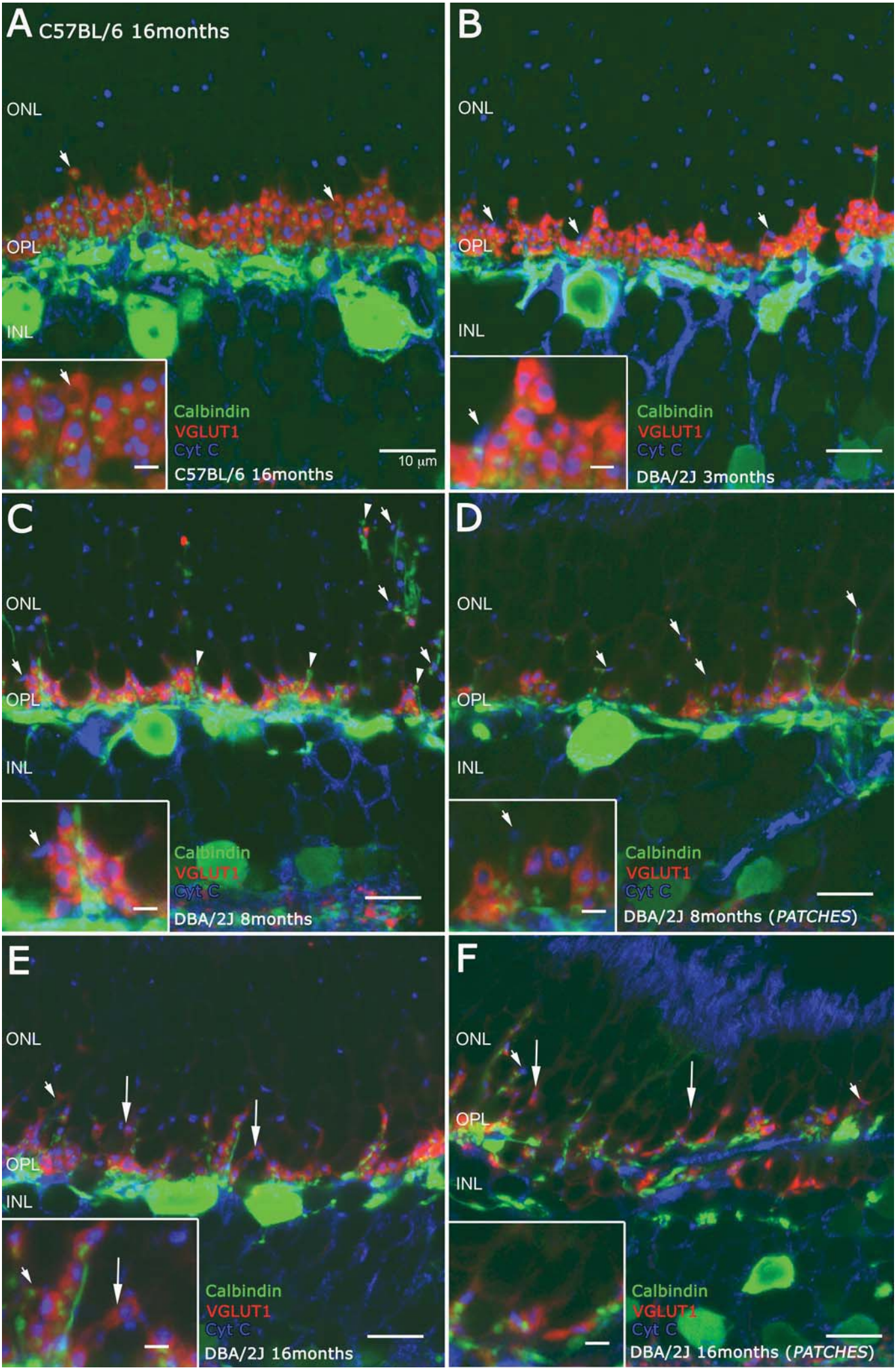
A C57BL/6 16months
ONL
OPL
INL
Calbindin
VGLUT1
Cyt C
C57BL/6 16months
10 µm
B
ONL
OPL
INL
Calbindin
VGLUT1
Cyt C
DBA/2J 3months
C
ONL
OPL
INL
Calbindin
VGLUT1
Cyt C
DBA/2J 8months
D
ONL
OPL
INL
Calbindin
VGLUT1
Cyt C
DBA/2J 8months (PATCHES)
E
ONL
OPL
INL
Calbindin
VGLUT1
Cyt C
DBA/2J 16months
F
ONL
OPL
INL
Calbindin
VGLUT1
Cyt C
DBA/2J 16months (PATCHES)

**Table 1.-** Primary antibodies used in this work.

| Molecular marker (Initials) | Antibody[(reference)] | Source and catalog number | Working dilution |
|---|---|---|---|
| Bassoon | Mouse monoclonal[51] | Stressgen (VAM-PS003) | 1:1000 |
| Calbindin D-28K (CB) | Rabbit polyclonal[48,60] | Swant (CB-38a) | 1:500 |
| C-terminal Binding Protein-2 (CtBP2) | Mouse monoclonal. Clone: 16/CtBP2[34] | BD transduction (612044) | 1:1000 |
| Cytocrome C | Mouse monoclonal, clone: 6H2.B4[61] | Zymed laboratories (33-8200) | 1:1000 |
| Guanine Nucleotide Binding protein 3 (GNB3) | Rabbit polyclonal[31] | Sigma (HPA005645) | 1:50 |
| Protein kinase C, α isoform (PKCα) | Rabbit polyclonal[60] | Santa Cruz Biotechnology (sc-10800) | 1:100 |
| Synaptophysin (SYP) | Mouse monoclonal, cone: SY38[60,19] | Chemicon (MAB5258) | 1:1000 |
| Syntaxin 4 (STX4) | Rabbit polyclonal[36] | Millipore (AB5330) | 1:500 |
| Transducin, Gαc subunit (Gt) | Rabbit polyclonal[62,60] | Cytosignal (PAB-00801-G) | 1:200 |
| Vesicular Glutamate Transporter 1 (VGLUT1) | Guinea Pig polyclonal[36] | Chemicon (AB5905) | 1 :1000 |
| Brain-specific homeobox/POU domain protein 3A (Brn-3a) | Goat polyclonal | Santa Cruz Biotechnology (sc-31984 L) | 1 :500 |